Proceedings of the 17th World Congress
The International Federation of Automatic Control
Seoul, Korea, July 6-11, 2008

Semi-Automated Control of AFM-based Micromanipulation using Potential Fields

Hamid Ladjal, Antoine Ferreira

PRISME Institute, ENSI de Bourges, Bourges, France.
(Tel: +332 4848 4079; e-mail: antoine.ferreira@ensi-bourges.fr).

Abstract: This paper proposes a truly interactive virtual environment (VE) system for 2-D assembly tasks at the microscale. It is based on the application of virtual potential fields as a control aid for performing safe and reliable path planning strategies. The planner covers a whole range of problems due to microscale effects in object assignment, obstacle detection and avoidance, path trajectory finding and sequencing. We investigated various paradigms for enabling the human operator and the automatic motion planner to cooperatively solve a motion planning task through the use of virtual potential fields. Communication between the operator and the planner is made through haptic/vision/sound modalities. First, we describe algorithms based on optimization theory and Voronoi graph construction taking into account the microscale effects. As automatic motion planners fail due to the difficulty of discovering critical configurations, we propose cooperation paradigms with operator skills in order to solve motion planning strategies. Then, potential fields are being used as a tool to generate velocity commands from an automatic path planner as well as allowing the human to interact. Finally, the ideas presented here are supported by experiments for efficient pushing-based manipulation constructing 2-D microparticle patterns.

1. INTRODUCTION

Recently, atomic forme microscopy (AFM)-based nanorobotic applications have been investigated with a great interest for fabrication of micro/nano electromechanical systems. As micromanufacturing process requires the sensing and positioning of complex micro-objects, motion planning and manipulation are challenging problems due to uncertain mechanics dominated by surface and intermolecular forces at microscale [1]. For parts with dimensions ranging from 150-10 μm, adhesive forces due to capillarity are dominant. It has been experimentally shown [2],[3] that assembly plans in the micro-domain are not reversible, motions required to pick up a part are not the reverse of motions required to release a part. As parts approach 1-10 μm or less, interactive forces such as van der Waals and electrostatic forces become major factors that greatly change the assembly sequence and path plans. Based on investigating the modeling of van der Waals forces as the dominant interactive microforce, the desirable trajectories of the end-effector of an AFM-robot [4] and path-planning strategies [5],[6] have been implemented and tested. However, building patterns with large numbers of microcomponents interactively is tedious and tends to be inaccurate, because humans have difficulties in performing precise positioning tasks. Thus, several human-machine interfaces (HMI) assisting AFM-based nanomanipulation systems have been developed in order to improve the reliability micro/nano manipulations tasks [7],[8],[9].

Automating the process of moving a large number of microcomponents in real-time is necessary to make such nanorobotic tasks possible. By following the generated motion paths, the tip can either follow the topography of the surface or move across the surface by avoiding collision with bumps. In [10], automatic strategies with vision-based controlled pushing techniques have been tested successfully for simple tasks. For complex 3-D planning tasks, the authors in [11],[12] developed specific heuristic algorithms. Different solutions have been proposed. Despite the large effort that has been spent on this problem, efficient fully automatic solutions at micro/nano scale work for very limited scenario.

Experience shows that automatic motion planners fail due to discovering critical configurations of the nanomanipulator that are in tight region or that are strongly influenced by the attractive/repulsive interaction microforces. In contrast, such critical configurations are often apparent to an operator. Similarly, Bayazit et al.[13] suggest that haptic feedback improves performance of path planners, and Taylor et al. [14] show that the haptic feedback is essential in finding the right starting position and guiding changes along a desired path during surface modification using Scanned-Probe Microscopes.

In this paper, we concentrate on designing a framework along a desired path in a real-time virtual environment (VE) for incorporating the strengths of both a human operator and an automatic path planning method to solve the complex strategy of automation at microscale. Virtual potential fields are proposed in order to provide an alternative for path planners during supervisory control, or when introducing 'hints' from human operator for haptically-generated paths. Potential fields are used because they provide a straightforward method which can incorporates efficient dynamic physically-based simulation (adhesive, repulsive, attractive microforces) in micro-environments without a set of a complex path planning rules. The VE system enhanced in this way will facilitate interactive

"damaging" tests of the path planning strategies. Section 2 gives an overview of the developed virtualized reality interface for tele-nanomanipulation. Section 3, shows how the micro/nano physics influence the trajectory planning of a cantilever tip when pushing an object. Then, integration in the virtualized environment (VE) of optimization algorithms using Voronoi graph construction and A* graph search are presented in Section 4. Finally, Section 5 presents human/planner cooperation using haptic and visual interfaces for human-centered micro-automation.

2. DESCRIPTION OF THE MUTISENSORY TELEMICROMANIPULATION SYSTEM

The description of the multisensory telemicromanipulation systems in given in Fig.1. It shows a multisensory human-machine interface (HMI) system connected to an AFM-based nanomanipulator working through the field of view of an optical microscope. In this work, it should noticed that the AFM equipment is not used for atomic-scale manipulation nor AFM-scanning mode. The nanomanipulator structure is composed of three linear translation stages (x,y,z) driven by DC motors for coarse motion (range: 8 mm, accuracy: 15 nm) combined with a 3 d.o.f ultra-high-resolution piezomanipulator (x,y,z) for fine positioning (range: 100 μm, accuracy: 1 nm). This hybrid nanopositioning system combines the advantages of ultra-low inertia, high-speed and long travel range. The end-effector is constituted by a piezoresistive AFM cantilever integrating a full-bridge strain gauge sensors.

The HMI is basically composed of virtual reality input/output devices connected to a virtualized reality interface (Fig.2). The goal of the developed human-machine interface is the improvement of the communication between the operator and the microenvironment through adequate interaction (haptic feedback, vision feedback and sound feedback). The multimodal HMI proposes assistance tools well adapted to the operational context of the micromanipulation tasks such as virtual metaphors, virtual fixtures and potential fields. As shown in Fig.2, the proposed interface is based on the virtualization concept of the microenvironment. It formulates the virtualized reality of the microenvironment through two sources of information (Fig.2): (i) from real image provided by optical microscopy and (ii) from synthetic views generated by a 3D model of the remote microworld. It reconstructs the scene, and manages microobject behaviors in the simulation loop while processing sensor data from the real world (the reader should refer to [9] for further explanations). The operator does not act directly on the real microscene but only on its virtual equivalent ensuring in this way a safe decoupling interface between the teleoperator (active part) and the microenvironment (passive part). The operator gestures are then retransmitted in real-time to the AFM-based manipulator according to the his manipulation skills.

During a working task, a working path is displayed on a graphic window which is shown in the virtual reality environment. Global path planning during pushing-based manipulation can be executed by the automatic planner and/or interactively by a human. A path planner generates automatically the global trajectory, while the human operator interacts haptically with the 3-D virtualized reality

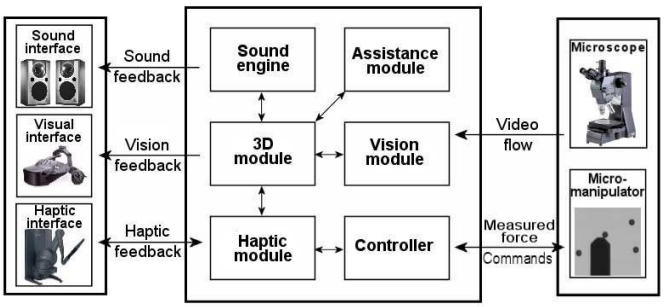

Fig. 1. Architecture of the multisensory telemicromanipulation system.

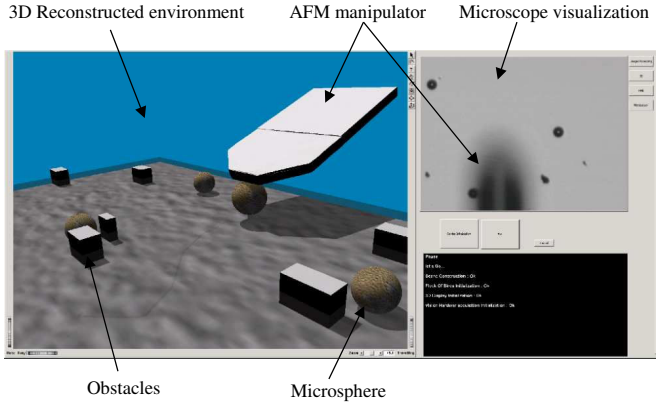

Fig. 2. Graphical user interface (GUI) integrating the real imaging (right side) provided the optical microscope and the reconstructed virtual microenvironment (left side) during real time AFM micromanipulation.

during pushing-based micromanipulation. These different issues are discussed in the following sections.

3. HUMAN/PLANNER COOPERATION USING ANTICIPATORY SYSTEM

In our previous works [9], teleoperated haptic path planning tasks have been tested successfully using haptic guides for 2-D path planning assistance. In this section we describe general ways where the human operator and the motion planner can work together to solve a planning and compliant motion control queries.

When the motion planner has generated the optimal path, the nanomanipulator go to the target location automatically through vision-based control. However, experience shows that unsuccessful actions occurs in critical configurations due to the interactive microforces and kinematic constraints. This suggests to design an anticipatory system in order to prevent some unsuccessful actions of the planner and unreliable commands which may cause failure of the whole task. In this way, the planner can help the operator by generating and controlling automatically the 'easy' portions of the path, and the operator creates collision-free paths from approximate paths generated by the planner using a haptic interface. The concept of anticipatory system which has been implemented is based on the definition of Rosen's theory [15] , as shown in Fig.3(a). It works as follows. The labels S, M, and E in the figure

stand for *object system*, *model*, and *effector*, respectively. In the Rosen's theory, S represents some dynamical system that interacts with the environment. M is a model of S. For a given state of S and an environement, M foretells what state S is likely to reach in the future. E is the effector that can interact with S or the environment in order to influence the future state of S.

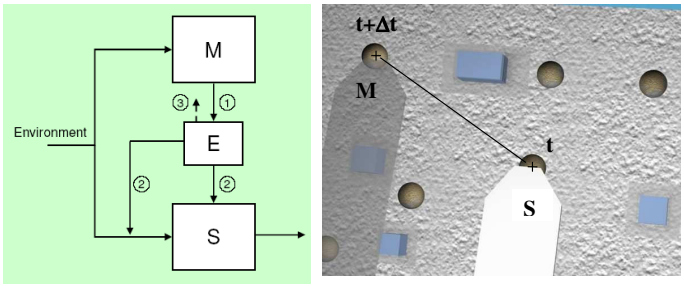

(a) (b)

Fig. 3. Anticipatory system for human/robot cooperation decision. (a) Rosen's anticipatory system scheme. M = Model, E = Effector, and S = Object System. (b) Application to the AFM-based nanorobotic system.

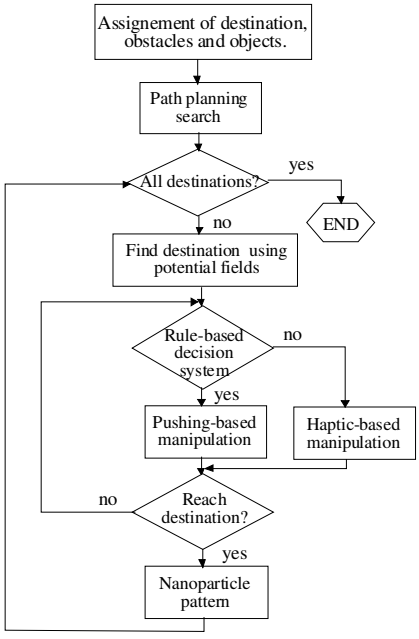

Fig. 4. Path planning strategy.

As illustration, Fig.3(b) gives an example of anticipatory micromanipulation task. We consider the dynamical system constituted by the end-tip of the AFM-based nanomanipulator (termed M), which is a model of the real AFM-robot (termed S). If the trajectories of S are parameterized by real time (t), then the corresponding trajectories of M are parameterized by a time variable which goes faster than real time (t+Dt). As S and M are starting at the same time in equivalent states during an equivalent time T, then M will proceed further along its trajectory than S. We can conclude that the behavior of M can predict the behavior of S in real-time. If we partitioned the workspace of S and M into regions corresponding to 'safe' and 'unsafe' states, the virtual AFM-robot M is used to detect

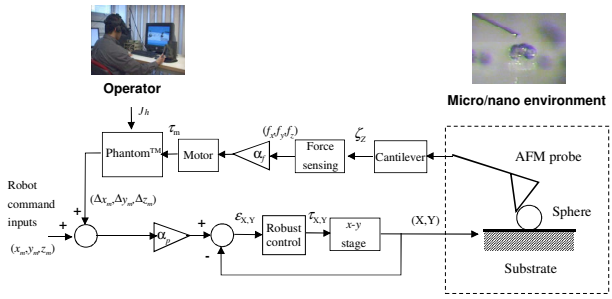

Fig. 5. AFM-based nanomanipulation system control.

the undesired regions and actions in order to avoid their occurrence in the real system S.

Basically, the proposed automatic task allocation will decide to allocate the next task to the machine or to the human operator based on their best expected performances. The path generation process of planning an AFM tip path is summarized in Fig.4. Every time the planner uses a vision-based control for pushing sequences, the generated commands to direct the AFM end-effector towards a location are first handled automatically by the anticipatory system. It simulates their execution in the virtual world, analyses the results and their impact on the task reliability and safety. Then, it decides whether to start executions in the real world or to alert the operator in order to handle the problem through haptic-generated paths. A reference model of successful evolution of planner actions is used through a rule-based decision system. From the evolution of the positions, contact forces, correlation between them, rules to identify a feasible and safe pushing are established. Unsafe regions or actions occurs when the AFM-tip can get stuck in a local minimum of potential field, may loose microparticles when turning around obstacles or apply excessive contact forces during pushing actions.

4. MOTION CONTROL STRATEGY

4.1 AFM-based Micromanipulation Control

To enhance the feeling of immersion, the operator can use a haptic interface (PhantomTM stylus) with 6-DOF positional input and 3-DOF force output for force-feedback interaction. Teleoperation control structure for PhantomTM device is given in (Fig.5). Bilateral teleoperation controller generates inputs for both slave and master manipulators in order to track scaled positions. Here, the operator is assumed to move smoothly and slowly for undesired instabilities. The operator controls the cantilever contact while feeling the normal interaction force between the AFM tip and the object. The aim of the teleoperation system is to track the robot command inputs x_m= (x_m, y_m, z_m) and/or master command inputs D_{xm}= (D_{xm}, D_{ym}, D_{zm}) in the microworld as x_s= (x_s, y_s, z_s).

The "ideal" controller response is given as

$$\begin{aligned} x_e &\rightarrow \alpha_p x_m \\ f_m &\rightarrow \alpha_f f_e \end{aligned} \tag{1}$$

Here, $\alpha_p > 0$ and $\alpha_f > 0$ are respectively the position and force scaling factor. As the controller, a force-reflecting servo type controller is selected where:

$$\begin{aligned} \tau_m &= -\alpha_f \ f_s - \ K_f(\ \alpha_f \ f_s - f_m) \\ \tau_s &= K_v \ (\ \alpha_p \ \dot{x}_m \ - \ \dot{x}_s) + K_p \ (\ \alpha_p \ x_m \ - \ x_s) \end{aligned} \tag{2}$$

where K_p and K_f are respectively the position and the force compensation gains. Thus, for enabling the ideal responses, K_p, K_f and α_p should be selected as large as possible.

4.2 Virtual Potential Fields for Global Motion

In our approach the robot is modeled as a particle acting under the influence of combination of two major potential fields $U(d)$ defined as:

$$U(d) = U_{att}(d) + \sum U_{rep}(d) \tag{3}$$

The goal of the first potential field, $U_{att}(d)$, is to attract the robot towards the final state. For that purpose, we assigned in the map a potential field which is defined as a crescent distance function from the final to the current state. The second component, $U_{rep}(d)$, is repulsive with a potential field inversely proportional to the distance from the obstacles. The fields can be modified by changing one or two variables which can makes them attractive for on-line modification by a human operator. The corresponding repulsive force is defined as the negative gradient of potential function, expressed as:

$$\overrightarrow{F}(d) = - \bigtriangledown U(d) \tag{4}$$

where ∇U_{global} represents the Laplacian operator.

According to the nature and the objective of the potential fields, we defined in the following several classes.

Potential field as attractive goal In order to assist the operator during object pushing motion, attractive potential fields have been implemented such as :

$$U_{att}(d) = \frac{1}{2}\xi \|d - d_{goal}\|^2 \tag{5}$$

$$F_{att}(d) = \xi \|d - d_{goal}\| \tag{6}$$

where d_{goal} is the goal position. As the parabolic function tends to zero at d_{goal}, the AFM-based manipulator gets closer to the goal configuration. The classical local minima problems associated with these attractive potential fields are avoided by operator manipulation skills during operation.

Potential fields as repulsive forces In order to guide haptically the operator gesture during pushing tasks, repulsive potentials are important in order to repel the AFM-based manipulator from a boundary which is not crossed. These repulsive potentials can also be used to constrain the involvement of the human. In order to avoid collisions with other objects and impurities, a repulsive boundary can be used to disallow the human maneuver the AFM-based manipulator outside a given workspace. The boundary is represented as an inverted rectangle expressed by:

$$U_{boun}(d) = A_b \frac{C_b(d)}{\exp^{-C_b(d)}} \tag{7}$$

$$C_b(d) = [(\frac{x - x_b}{a_b})^{2d} + (\frac{b_b}{a_b})^2(\frac{y - y_b}{b_b})^{2d}]^{\frac{1}{2d}} - 1 \tag{8}$$

where A_b is a scaling factor and $C_b(d)$ is expressed by:

where x_b and y_b specify the center of the rectangle. The dimensions a_b and b_b are derived from the width w and depth z of the rectangle, calculated as follows:

$$a_b = \frac{w}{2}(2^{\frac{1}{2d}}) \quad and \quad b_b = \frac{z}{2}(2^{\frac{1}{2d}}) \tag{9}$$

During telemicromanipulation tasks, the operator can potentially collide with dust and/or sphere particles which are present in the configuration space. Owing to the dust physical interaction properties (electrostatic force, van der Waals force and adhesive force), attractive forces can greatly disturb the manipulation operations. To deal with the problem of real-time collision-free path planning, virtual repulsive forces are generated around obstacles from discrete potential fields. The expression of this potential field is given as follows (Fig.**??**):

$$U_{obstacle}(d) = \begin{cases} \frac{1}{2} \ \eta \ (\ \frac{1}{d} \ - \ \frac{1}{d_0} \ ) & if \ d \ \leq \ d_0 \\ 0 & if \ d \ > \ d_0 \end{cases} \tag{10}$$

where d, d_0 and η represent the penetration distance, the positive constant and the position scaling factor.

The combination of 2-D path planning optimization and the attractive and repulsive virtual potential fields gives a potential field map (Fig.7) for operator haptic guidance during pushing tasks. The idea of this kind of assistance fixture is to achieve guided motion paths of the AFM tip without touching the obstacles. Its role is to prevent the attraction of the AFM tip from the micro-objects under the adhesion forces (van der Waals force, electrostatic force, surface tension force). This virtual guide appears as an elastic mechanical impedance created at the contact moment between the AFM tip and the geometrical representation of the potential field.

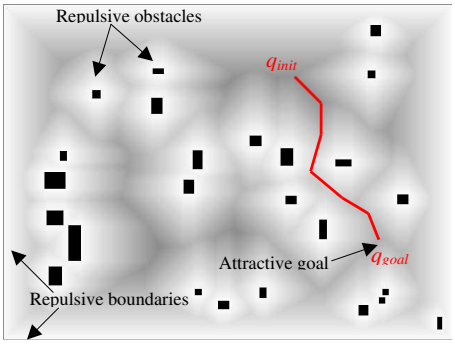

Fig. 7. C-Space distribution of repulsive and attractive virtual potential fields. A virtual fixture is overlaid on the virtual environment for operator gesture guidance during micromanipulation tasks.

4.3 Micromanipulation using Sliding Mode Controller

As a geometrical constraint in the task space configuration manifold (C-Space), the fixture imposes restrictions to

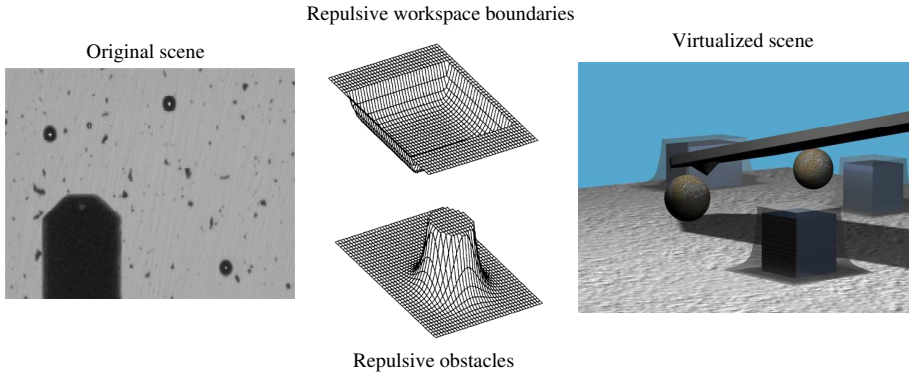

Fig. 6. Haptic and VR interfaces for real-time human/planner cooperation using potential fields for micromanipulation. (a) real images from the microscope; (b) Integration of repulsive force fields for boundary of the workspace and microsphere obstacle for guidance of planning microtasks and (c) 3D representation in a virtual environment.

the robot movements, thus ensuring that the AFM-based robotic manipulator does not collide with the microobject. Although their control properties have not been studied, the virtual fixture can be abstracted as a sliding surface. Here, a point in the C-Space that represents the configuration space of the AMF probe can move (or slide) along the sliding surface toward the goal defined by the attractive potential field defined in [16]).

4.4 Haptic-based Manipulation using Multisensory Feedback

Through interaction using the haptic interface, the operator is able to slide along the surface during pushing-based micromanipulation along the surface toward the goal while feeling the virtual reaction force normal to this surface. The key requirement for application of the virtual fixture is microtask dependency, which has a major influence on its implementation.

A potential field surrounds the handled microspheres with a spherical geometry acting as a shock absorber potential field given as follows :

$$U_{sphere}(d) = \begin{cases} \lambda \dfrac{\delta d}{\delta t} & if\ d \leq d_0 \\ 0 & if\ d > d_0 \end{cases} \qquad (11)$$

where δ is the partial derivative and λ is a position scaling factor.

Its simple geometry possess the advantage of being symmetrical and continuous in 3-D space which minimizes the risks of gesture jump.

When the AFM probe closely approaches the micro-sized object, visible resolution of 3-D optical microscope is limited to observe the interaction, the user interface gives warning messages offering the sound feedback to the operator. At the contact point, the user interface offers force feedback through the haptic interface. The main components of the adhesion forces f_{adh} (van der Waals and adhesive) between an AFM cantilever and micro-sized object are given in detail in [2].

4.5 Experiments and Conclusion

The developed algorithm has been implemented and tested for the generation of the optimized path to manipulate microparticles. The easy portions of the paths are controlled automatically through vision-based control.

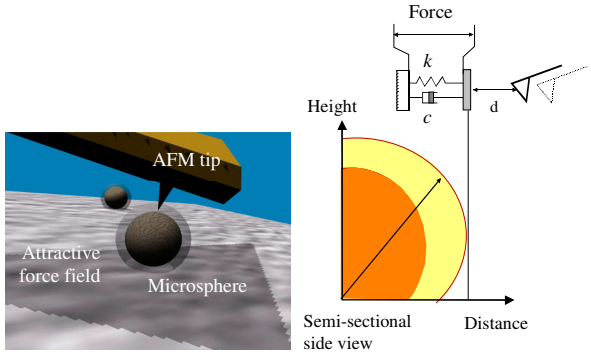

Fig. 8. The repulsive potential field: (a) Manipulation with potential fields, (b) repulsive potential field representation.

When the AFM-tip is close to critical configurations due to obstacles, the rule-based decision system noticed some disturbance forces. At this query, the operator decided to help the planner with the aid of the haptic interface. The transition to switch to the semi-autonomous mode is initiated manually when the operator applies the corresponding forces on the haptic interface. We collected statistics regarding quantities to relate to planning difficulty while the human operator was guiding the AFM-based robot through the 3D virtual environment. The particular quantities we considered are the number of collisions, the robot's distance from the nearest obstacle, and the magnitude of the robot's reactive forces. Two family of tests have been performed: (i) vision and force modalities (V+F) (see Fig.9(a)) and (ii) vision, force and auditory modalities (V+F+A) (see Fig.9(b)).

These experiments call for different comments.

- In Fig.9(a), the reactive force acting on the robot was measured every time the robot collided with an obstacle. The results reinforce our intuition. As we can notice, the path for the AFM-based robot driven along the optimized trajectory by the operator through the haptic interface, contains no collisions in the beginning and then fewer collisions occurs with the virtual repulsive obstacles. Similarly, the separa-

tion distance maintained between the AFM and the nearest obstacle which fluctuates very slowly. Note that the both plots show similar patterns over time. Finally, the analysis of reactive forces shows that the operator had some difficulties in maneuvering the AFM-based robot in very narrow configurations due to non-holonomic constraints and limited degrees of freedom. However, several experiments shown that the number of collisions is strongly reduced when considering the optimal path proposed in the previous planning method compared to an intuitively (approximate) one.

- In Fig.9(b), the results shows a general diminution of the number of contact collisions and magnitude of rendered force when considering an extra auditory modality.

When the operator judges that no critical situations appear, he releases the control to the remote controller. Critical situations can be avoided with the aid of human manipulation capabilities. The process continue until all destinations are performed.

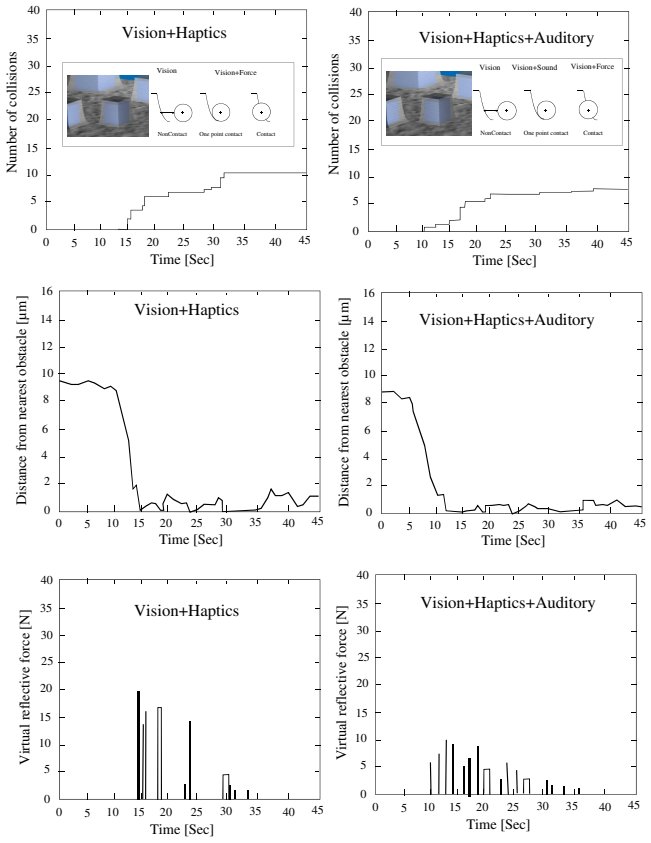

Fig. 9. Experimental graphs depicting time versus total collisions, AFM-based manipulator's clearance defining the distance with the obstacle, and contact force acting on the nanomanipulator : (a) with vision+haptics and (b) with vision+haptics+auditory feedbacks.

REFERENCES

[1] J. Israelachvili, Intermolecular forces, *IEEE Transactions on Mechatronics*, 2nd Edition, Academic Press, San Diego, 1992.

[2] M. Sitti, Controlled Pushing of Nanoparticles: Modeling and Experiments, *IEEE/ASME Trans. on Mechatronics*, vol.5, No.2, June 2000, pp. 199-211.

[3] Ferreira A., Cassier C. and Hirai S. , Automatic Microassembly System Assisted by Vision Servoing and Virtual Reality, *IEEE/ASME Trans. on Mechatronics*, Vol.9, No.2, June 2004, pp.321-333

[4] Li Guangyong, Xi Ning, Wang Yuechao, Yu Mengmeng, Fung Wai-Keung, Planning and control of 3-D nanomanipulation, *Acta Mechanica Sinica*, Volume 20, Number 2, sep. 2006.

[5] D-H. Kim, T.Kim, K.Kim, B.Kim, Motion Planning of an AFM-based Nanomanipulator in a Sensor-based Nanorobotic Manipulation System, *3rd Int. Workshop on Microfactories*, Minnesota, Sep. 2002.

[6] John T. Feddema, Patrick Xavier and Russell Brown, Micro-assembly planning with van der Waals force , *J. of Micromechatronics*, Vol.1, No.2, pp. 139-153, 2001.

[7] G.Li, N.Xi, M.Yu, W-K.Fung, Development of Augmented Reality System for AFM-based Nanomanipulation, *IEEE/ASME Trans. on Mechatronics*, Vol.9, N.2, June 2004, pp.358-365.

[8] W.Vogl, B. Kai-Lam Ba, M.Sitti, Augmented Reality User Interface for an Atomic Force Microscope-based Nanorobotic System, *IEEE Trans. on Nanotechnology*, Vol.52, No.6, December 2005, pp.1506-1520.

[9] M. Ammi, A.Ferreira, Virtualized Reality Interface for Tele-Micromanipulation, *IEEE ICRA*, New Orleans, LA, pp.577-582, 2004.

[10] N.A. Lynch, C.Onal, E.Schuster, M.Sitti, A Strategy for Vision-Based Controlled Pushing of Microparticles, *IEEE Int. Conf. on Robotics and Automation*, Roma, Italy, 10-14 April, pp.1413-1418, 2007.

[11] J.H. Makaliwe, A.A.G. Riquicha, Automatic Planning of Nanoparticle Assembly Tasks, *IEEE Int. Symp. on Assembly and Task Planning*, Fukuoka, Japan, May 28-30, pp.288-293, 2001.

[12] O. Ben-Shahar, E.Rivlin, Practical Pushing Planning for Rearrangement Tasks, *IEEE Trans. on Robotics and Automation*, Vol.14, No.4, pp.549-565, 1998.

[13] O.B. Bayazit, G.Song, N.M. Amato, Enhancing Randomized Motion Planners: Exploring wit Haptic Hints, *IEEE Int. Conf. On Robotics and Automation*, San Francisco, CA, pp.529-536, 2000.

[14] P. Bhatia, M. Uchiyama, A VR-Human Interface for Assisting Human Input in Path Planning for Telerobots, *Presence*, Vol.8, No.3, 1999, pp.332-354.

[15] R. Rosen, Anticipatory Systems: Philosophical, Mathematical and Methodological Foundations, *Pergamon*, NY, 1985.

[16] Y. B. Shtessel, Nonlinear output tracking in conventional and dynamic sliding manifolds, *IEEE Trans. on Automatic Control*, Vol.42, No.9, pp.1282$_1$286, 1997.